

Supplemental Information

Direct Medial Entorhinal Cortex Input to Hippocampal CA1 is Crucial for Extended Quiet Awake Replay

Jun Yamamoto and Susumu Tonegawa

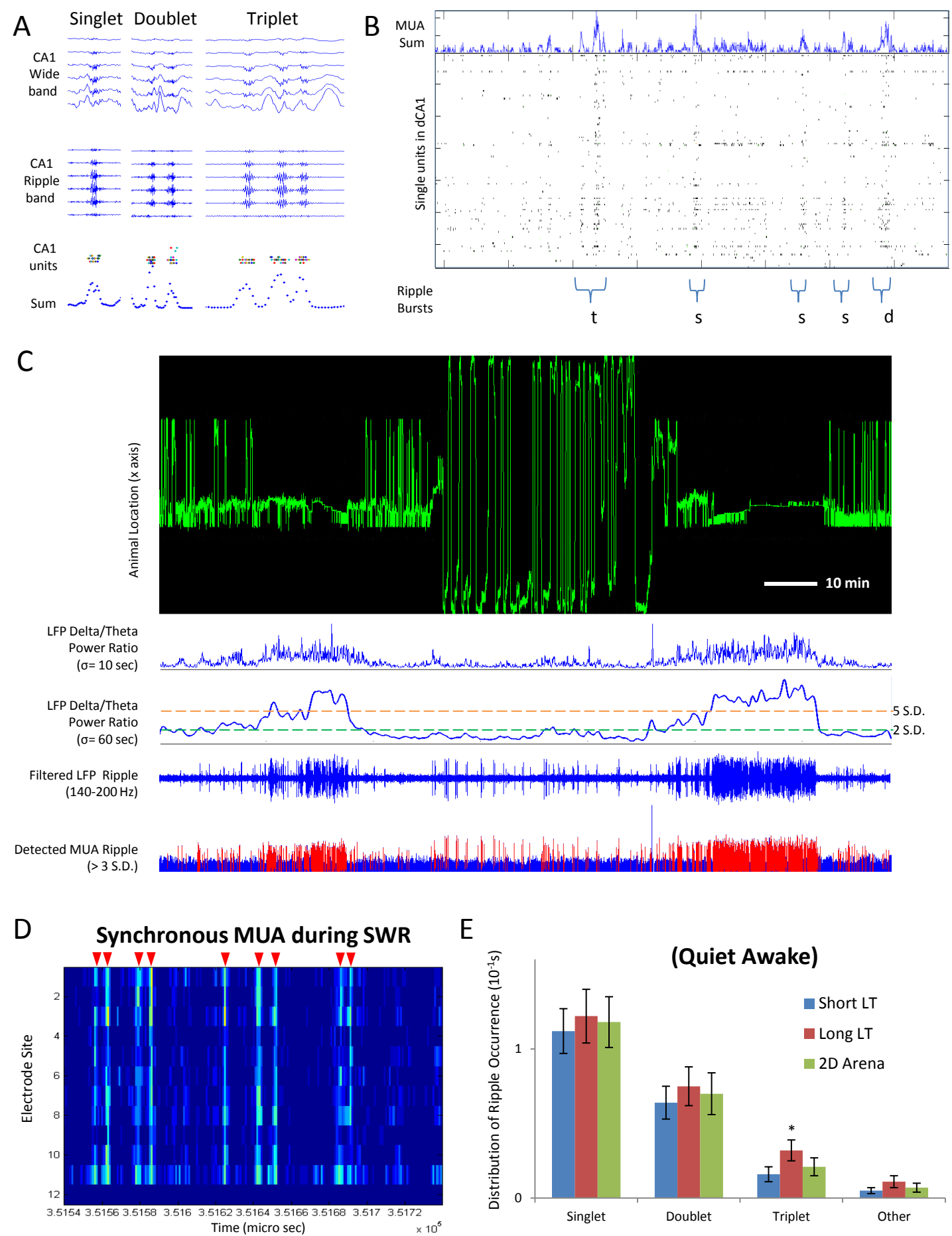


Figure S1

Figure S1. Examples of Hippocampal Ripple Bursts

- (A) Another examples of single ripple and ripple bursts (doublet and triplet) measured with silicone linear probes covering stratum oriens, pyramidal cell layer and stratum radiatum area of CA1 area. Top panel: Wideband signal in CA1. Middle panel: Ripple band (150-200 Hz) oscillation recorded in CA1. Bottom panel: Recorded CA1 multi-unit spiking activity and its sum.
- (B) An example of ripple bursts plotted with MUA and extracted single unit activities.
- (C) General recording scheme of this study. Top panel: Linearized animal position during pre-run, run, post-run periods. Bottom panel: Delta/Theta power ratio (smoothing kernel: $\sigma = 10$ sec), Delta/Theta power ratio (smoothing kernel: $\sigma = 60$ sec) with 2 S.D. and 5 S.D. threshold for sleep classification, Filtered ripple-band trace and detected MUA ripple using 3 S.D. threshold.
- (D) An example of synchronized MUAs during sharp-wave ripples (SWRs) recorded in dorsal CA1. This example illustrates that most of the recording sites becomes precisely highly active during SWRs (bin size: 10 ms).
- (E) Distribution of ripple occurrence per ripple burst types in short / long / 2-D arena. Singlet: Short LT: 1.12 ± 0.15 ($10s^{-1}$) / Long LT: 1.22 ± 0.18 ($10s^{-1}$) / 2D Arena: 1.18 ± 0.17 , $P_{\text{single}} = 0.552$, one-way ANOVA, Doublet: Short LT: 0.64 ± 0.11 ($10s^{-1}$) / Long LT: 0.75 ± 0.11 ($10s^{-1}$) / 2D arena: 0.70 ± 0.14 , $P_{\text{double}} = 0.268$, one-way ANOVA, Triplet: Short LT: 0.16 ± 0.05 ($10s^{-1}$) / Long LT: 0.32 ± 0.07 ($10s^{-1}$) / 2D arena: 0.21 ± 0.06 , $*P_{\text{triple}} = 0.041$, one-way ANOVA Other: Short LT: 0.05 ± 0.02 ($10s^{-1}$) / Long LT: 0.11 ± 0.04 ($10s^{-1}$) / 2D arena: 0.07 ± 0.03 , $P_{\text{other}} = 0.482$, one-way ANOVA.

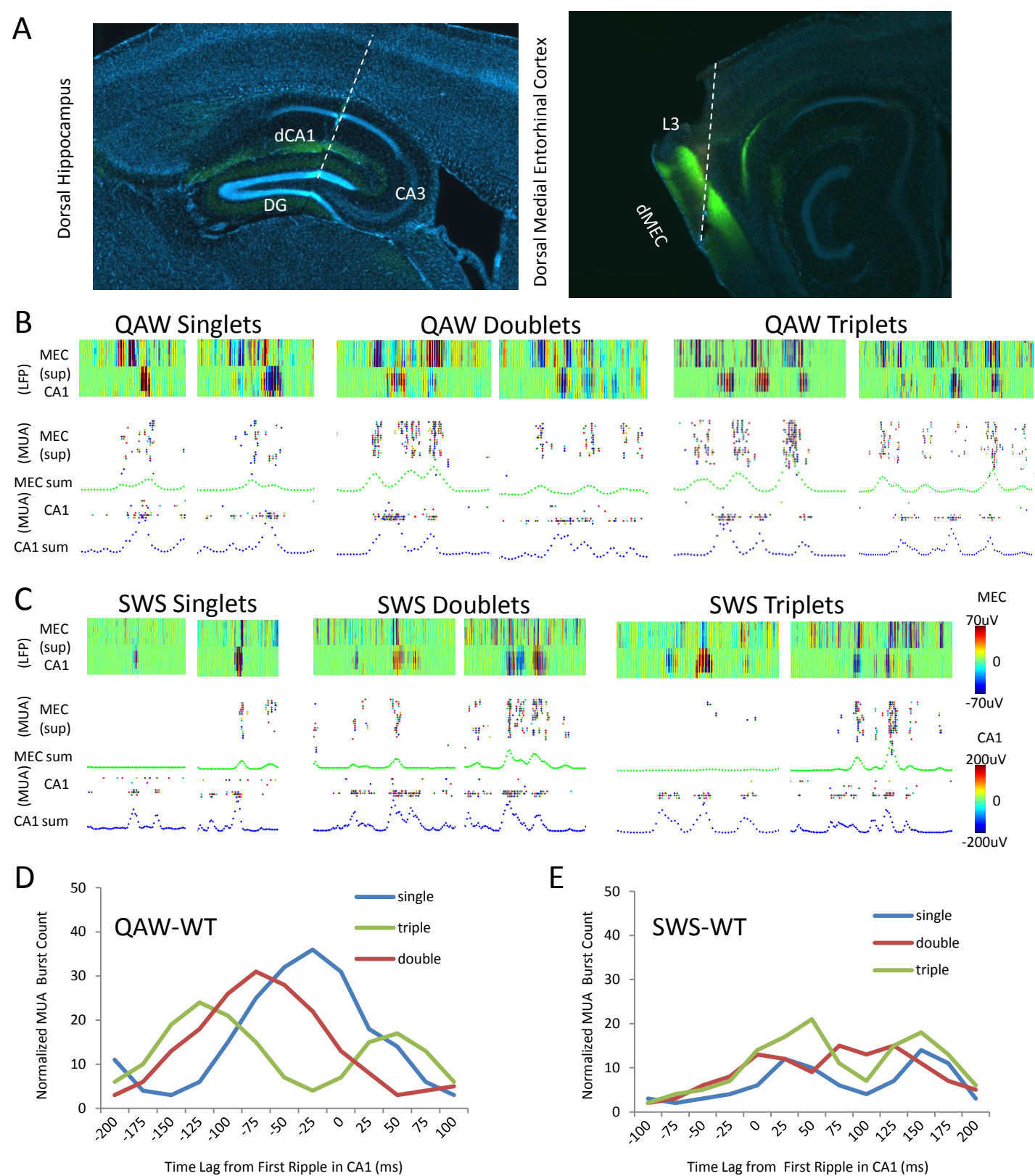


Figure S2

Figure S2. Recording Sites and More Examples of the Ripple Bursts in Both QAW and SWS

- (A) Histology of the silicone probe dual-site recordings. Green signals are from AAVrh8-DIO-eArchT-eYFP virus expressed in stratum lacunosum moleculare. area in dCA1 and MEC layer III in dMEC.
- (B) More examples of ripple bursts from 2nd and 3rd animals. Format same as in Figure 2A and 2B during QAW.
- (C) Same as in Figure 2D during slow-wave sleep (SWS), but from 2nd and 3rd animals. (note: MEC's LFP amplitudes were much lower (three folds) than that of CA1's due to referencing in MEC area).
- (D) Distribution of temporal lags between preceding MEC burst and CA1 ripples during QAW. First ripple was used in ripple bursts (doublets and triplets).
- (E) Same as in (D) but during SWS.

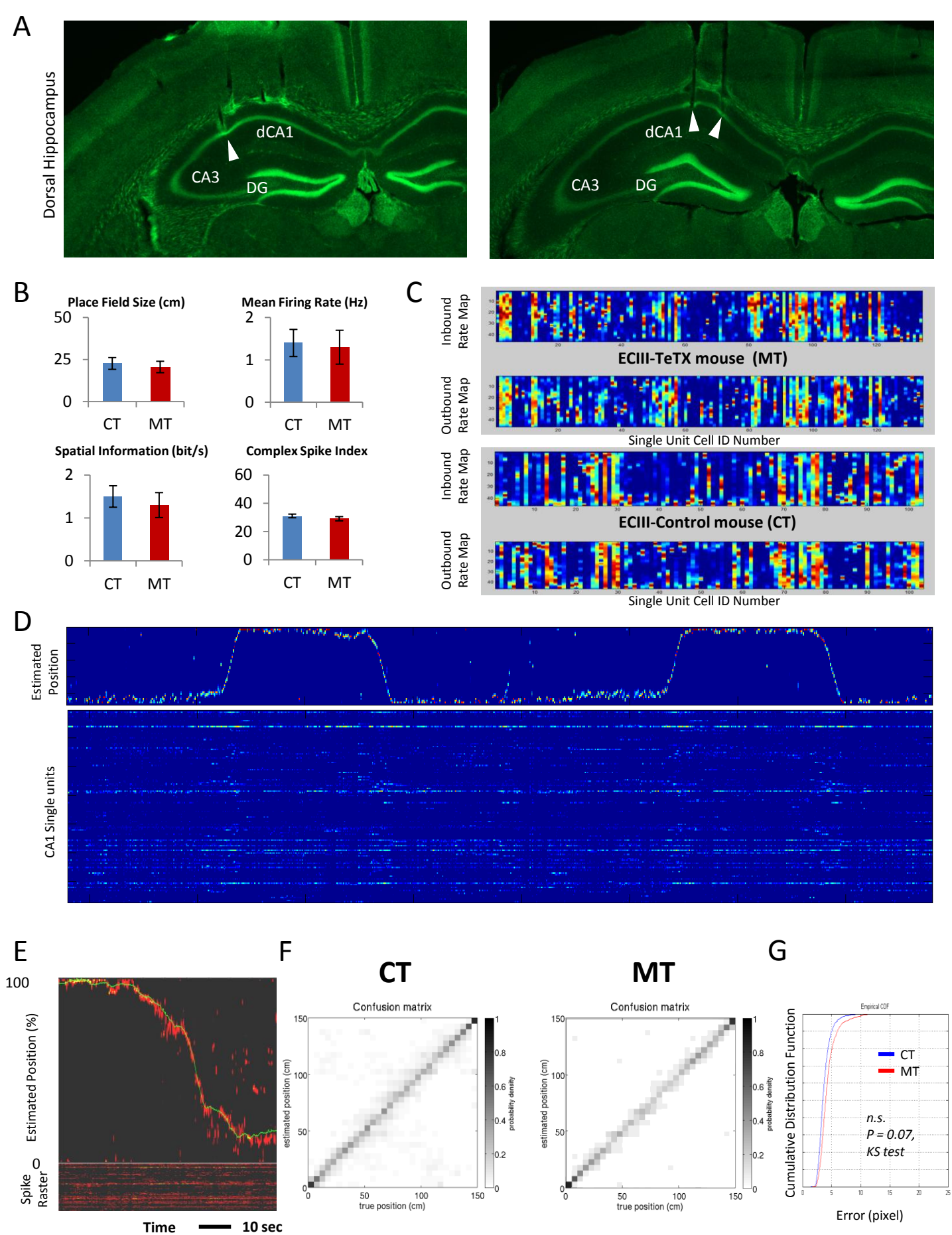
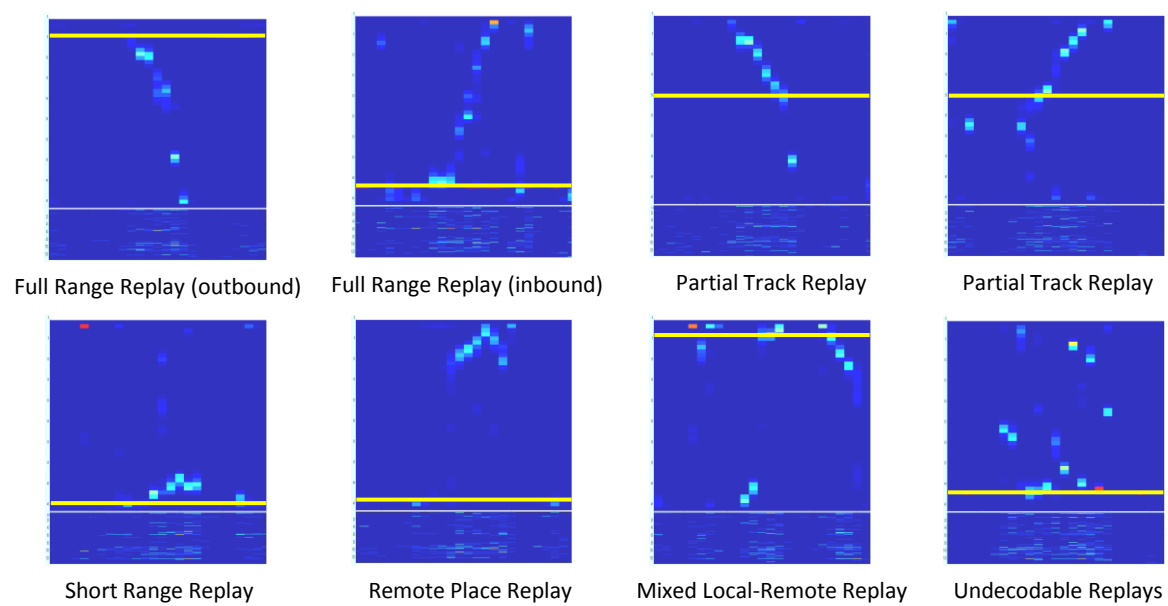


Figure S3

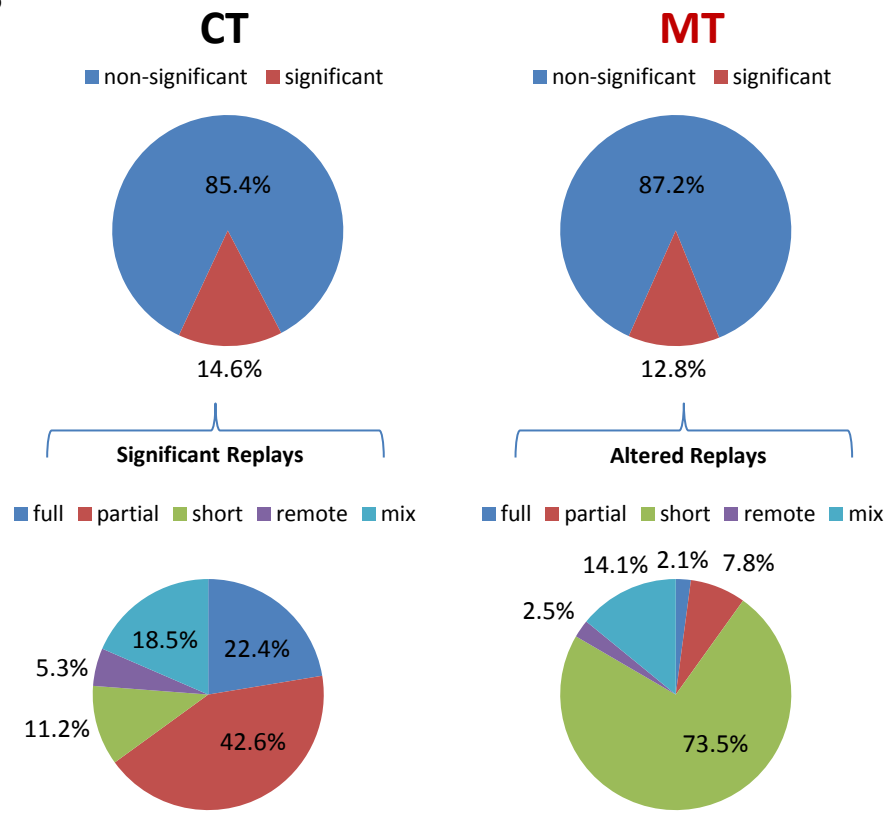
Figure S3. Comparable Decoding Results during Awake RUN

- (A) Histology of the large-scale tetrode recordings.
- (B) No significant differences were observed between CT and MT mice in place field size (CT: 35.6 ± 5.3 %, MT: 38.2 ± 6.2 %), paired t test, $t(432) = 1.279$, $P = 0.204$, mean firing rate (CT: 1.52 ± 0.25 Hz, MT: 1.33 ± 0.29 Hz) paired t test, $t(432) = 0.613$, $P = 0.558$, spatial information (CT: 1.44 ± 0.32 bits/spike, MT: 1.31 ± 0.42 bits/spike) paired t test, $t(432) = 0.539$, $P = 0.068$ and complex spike index (CT: 31.4 ± 1.3 , MT: 29.1 ± 1.5) paired t test, $t(432) = 0.228$, $P = 0.836$.
- (C) Examples of spatial receptive fields of isolated units from MECIII-TeTX MT and CT mice. X-axis: single unit ID number, Y-axis: firing location. Both putative excitatory and inhibitory units are included.
- (D) Example of decoding results in CT mice during RUN session. Top panel: Decoded position based on large scale single units from CA1. Warmer color represents higher probability. Bottom panel: Rate map of binned single unit activities. Decoding bin size for RUN: 200 ms.
- (E) Example of RUN decoding results in MECIII-TeTX MT mouse. Top panel shows estimated position and true position from the video tracking system. Bottom panel shows corresponding single unit activities.
- (F) Examples of confusion matrix from MECIII-TeTX MT and CT respectively. Darker pixel denotes higher accuracy of the decoding result.
- (G) Cumulative distribution function of replay positional error $P = 0.065$, K -S test.

A



B



C

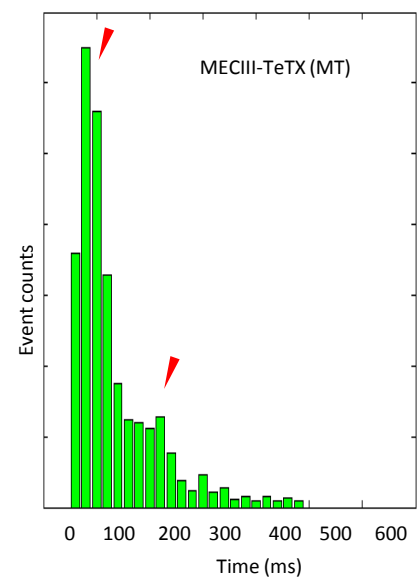


Figure S4

Figure S4. Various Replay Coverage in MECIII-TeTX MT and CT Mice

- (A) Examples of eight different types of replay spatial coverage. Each panel represent statistically significant replay event. Categorization used here are Full Range (covers more than 80% of length of a track), Partial (covers between 20-80%), Short (less than 20%) and Remote (less than 40% of coverage and more than 50% away from current position). Yellow lines represent current position at the time of replay event. Mix and Undecodable events do not pass bootstrap test.
- (B) A breakdown chart of replay types between MECIII-TeTX MT and CT. Top panel: Proportion of statistically significant replays CT: 14.6%, MT: 12.8%. Bottom panel: A breakdown chart of replays by type CT: Full: 22.4%, Partial: 42.6%, Short: 11.2%, Remote: 5.3% and Other: 18.5%, MT: Full: 2.1%, Partial: 7.8%, Short: 73.5%, Remote: 2.5% and Other: 14.1%.
- (C) Same as in Figure 1G but in MECIII-TeTX mutant. Red arrowheads denote local peaks (around 80, 170 ms) in the monotonous Poisson distribution.

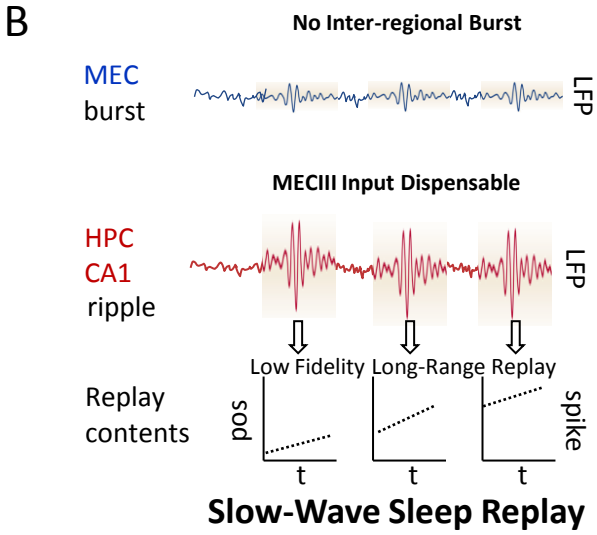
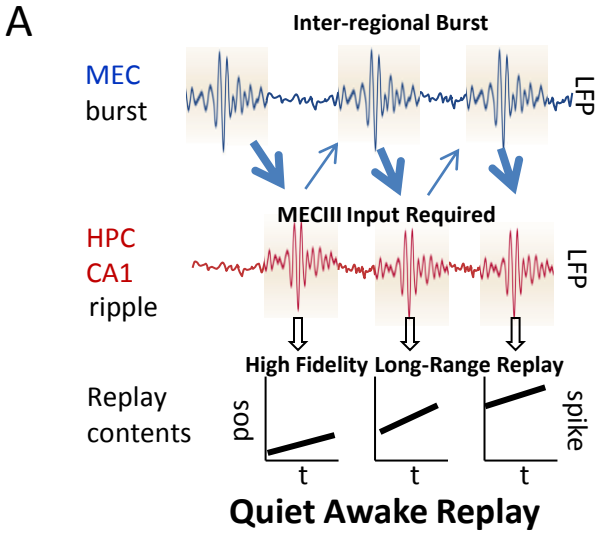


Figure S5

Figure S5. A Summary Cartoon of Our Findings

- (A) During QAW, alternating ripple burst activities, which requires MECIII input, were observed between superficial layers of MEC and dorsal CA1. The replay quality (fidelity) was high.
 - (B) During SWS, no inter-regional alternating ripple activities observed. The replay quality was low.
- .